A Novel Method for Quantifying Arm Motion Similarity

Zhi Li[1], Kris Hauser[1], Jay Ryan Roldan[2], Dejan Milutinović[2], and Jacob Rosen[3]

Abstract— **This paper proposes a novel task-independent method for quantifying arm motion similarity that can be applied to any kinematic/dynamic variable of interest. Given two arm motions for the same task, not necessarily with the same completion time, it plots the time-normalized curves against one another and generates four real-valued features. To validate these features we apply them to quantify the relationship between healthy and paretic arm motions of chronic stroke patients. Studying both unimanual and bimanual arm motions of eight chronic stroke patients, we find that inter-arm coupling that tends to synchronize the motions of both arms in bimanual motions, has a stronger effect at task-relevant joints than at task-irrelevant joints. It also revealed that the paretic arm suppresses the shoulder flexion of the non-paretic arm, while the latter encourages the shoulder rotation of the former.**

I. Introduction

Bimanual arm motions are characterized by temporal and spatial coupling, due to which the arms tend to move symmetrically [1]–[3]. For stroke patients with motor disability (i.e., hemiparesis), inter-arm coupling tries to synchronize the paretic arm with the non-paretic arm despite of deteriorated motor function, which might aid recovery [4]. Studies of chronic stroke patients have shown that the peak velocities of the paretic arm were increased in symmetrical bilateral motions, at the expense of deteriorated performance of the non-paretic arm [5], [6]. Due to inter-arm coupling, the paretic arm may improve its motor function by moving with the non-paretic arm, which has been reported in a therapy with symmetrical exercises (e.g., Bobath neuro-developmental approach) and other bilateral training therapies [7]–[10].

The neural mechanisms of human motor control have been investigated (for comprehensive review see [11]). However, clinical studies still argue whether bilateral training is more effective than alternative therapies [12], [13], mostly due to the lack of a consistent measurement that can compare motor function recovery across therapies that differ in their tasks. Previous research efforts on the symmetry of bimanual motions compare arm motions either using the kinematic/dynamic variables of the two arms (e.g., motion timing, hand trajectory, muscle activity, etc.), or by various task-dependent performance indexes (e.g., the aspect ratio for circle drawing tasks) [14]–[21]. Due to differences in tasks, these measurements of kinematic/dynamic variables cannot be directly compared across studies.

This paper proposes a method to quantify the motion similarity of two arms regardless of the task, which is generally applicable to any kinematic and dynamic variables of interest. The idea behind the method is to map two motions against one another, and quantify the similarity and complexity of the mappings via four real-valued feature variables. For both in-phase and anti-phase motions, the extracted feature variables can characterize the motion similarity of two arms, as well as of the same arm across trials. To validate the utility of these features, data was collected from chronic stroke patients on unimanual and bimanual motions of identical tasks. The features were applied to quantify mapping similarity between arms, and on the same arm in both the bimanual and unimanual conditions. The features are sufficiently sensitive to indicate the behavior changes of the non-paretic and paretic arms, and suggest that the effect of inter-arm coupling is stronger on the task-relevant joints than the task-irrelevant joints in symmetric arm motions.

II. Methodology

A. Quantification of Motion Similarity

The proposed method uses three mapping symmetry features and one mapping complexity feature to quantify the similarity of two motions. First, a kinematic/dynamic feature (e.g., joint angle) of one motion is plotted against the other motion with correspondences determined along a normalized time dimension. Fig. 1 shows the mapping of joint angles (denoted by θ_i and $\theta_i^{'}$) between two motions. Next, linear regression is used to find the **the absolute value of the slope** $\mathbf{p_1}$ and the **intersection** $\mathbf{p_2}$ for the mapping (i.e., $\theta_i^{'} = p_1\theta_i + p_2$). The coefficient of determination $\mathbf{R^2}$ is computed, referred as the **mapping linearity**. Note that $p_1 \in [0, +\infty]$,$p_2 \in [-\infty, +\infty]$, and $R^2 \in [0, 1]$. For ideally symmetric motions, the mapping plots are straight line segments with $p_1 = 1$, $p_2 = 0$ and $R^2 = 1$. Larger deviations from these values indicate less motion similarity. The last feature measures **mapping complexity** $\mathbf{N_c}$. Mappings of similar motions (in-phase or anti-phase) are well approximated by a single line, while more complex mappings would require multiple line segments to achieve tolerable accuracy. This feature measures how many line segments are needed for fitting the mapping with a pre-determined accuracy level.

Fig. 1a to 1c illustrate the significance of each mapping symmetry feature. For a mapping of two motions, p_1 indicates which motion traverses more of the joint space. Different average postures between two motions result in a non-zero p_2, while nonlinear deviations make $R^2 < 1$.

[1]Zhi Li zhi.li2@duke.edu and Kris Hauser kris.hauser@duke.edu are with Electrical & Computer Engineering Department, Duke University, Durham, NC, 27708, USA.

[2]Jay Ryan Roldan juroldan@ucsc.edu and Dejan Milutinović dejan@soe.ucsc.edu are with the Department of Computer Engineering, University of California, Santa Cruz, Santa Cruz, CA, 95064, USA.

[3]Jacob Rosen is with Department of Mechanical & Aerospace Engineering, University of California, Los Angeles, Los Angeles, CA, 90095, USA rosen@seas.ucla.edu

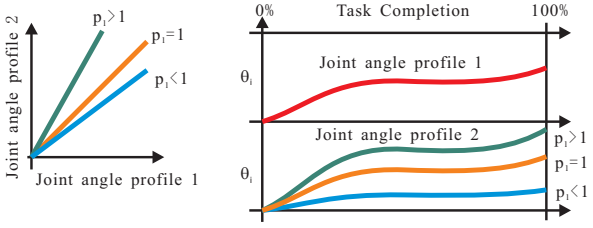

(a) p_1 - diverging trajectories result in different slopes

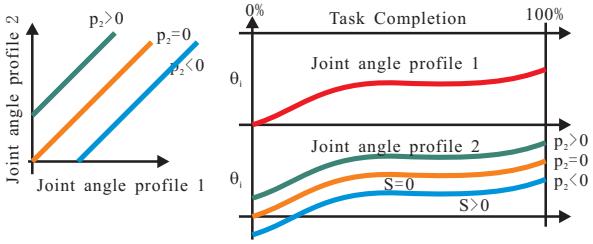

(b) p_2 - parallel trajectories result in different intersections

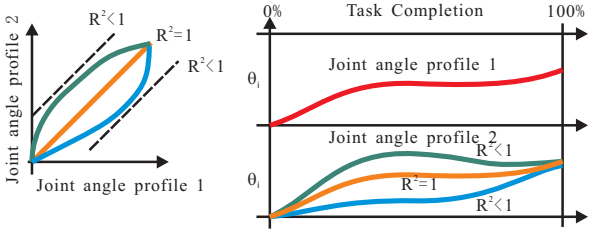

(c) R^2 - nonlinear deviations influence mapping linearity

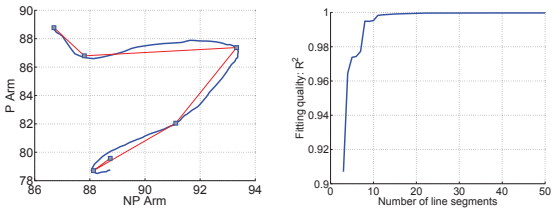

(d) N_c is the mapping complexity resulting from piecewise linear fitting. More line segments are needed by approximation of higher fitting quality.

Fig. 1: The mapping symmetry and complexity features.

For inter-arm mappings, mapping symmetry features indicate motion differences between the arms. For mappings between unimanual and bimanual motions, these features measure arm behavior changes due to inter-arm coupling. In Fig. 1d, piecewise linear regression is applied to an inter-arm mapping for the elbow flexion θ_4 of a stroke patient. As the number of line segments necessary (denoted by N) goes up, the fitting quality increases and eventually stabilizes (refer to Fig. 1d). To represent the shape of a mapping plot without over-fitting, the mapping complexity N_c is defined as the smallest N with coefficient of determination of the piecewise linear fitting larger than some threshold α (α was chosen to be 0.95 throughout this paper). The mapping complexity of two motions reflects the difficulty in generating one motion given the knowledge of the other. It is similar to the mapping linearity feature R^2, since the mismatching of two motions results in more turning points in the mapping plot and thus more approximation segments, yet a mapping plot that consists of a few largely non-collinear segments may have large mapping linearity but low mapping complexity.

B. Subjects, Protocol and Experimental Setups

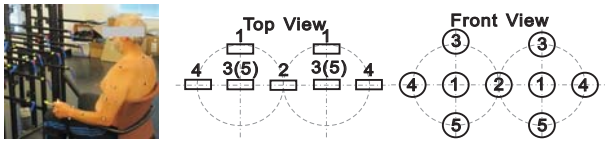

(a) (b)

Fig. 2: In reaching experiments, (a) passive reflective markers are attached to the arms and torso of the subjects for position tracking; (b) targets for each hand are aligned on circles centered on the subject's shoulders.

The data for this study were collected from eight chronic stroke patients, ranged in age from 53 to 72 years old (average 60.4 ± 7.2). Among the eight subjects, six were impacted on the right arm and two on the left arm. Subjects scored between 20 and 27 on the upper limb volitional motion portions of the Fugel-Meyer assessment, out of a total score of 30. Fig. 2a depicts the workspace setup of the experiment. As shown in Fig. 2b, the left/right targets are arranged on the surfaces of spheres corresponding to the left/right hand of the subject. The center and radius of the two spheres are adjusted according to the shoulder width and height of the subject to align Target 1 in each sphere with the corresponding shoulder. The distance between the subject and the workspace is adjusted such that the subject can reach each target comfortably. During the experiment, the subject starts from resting their arms on the handle of the chair, with consistent wrist positions. At a "go" command, the subject starts reaching for the instructed target, touching the target with the tip of the tool held in hand. The experiment consists of two unimanual sessions and one bimanual session. In the unimanual sessions, the subjects reach with their left/right hand to the five targets corresponding to that hand. In the bimanual session, the subjects reach for both the left and right targets symmetrically. Each session consists of 25 individual trials (5 targets $\times$ 5 repetitions). A motion capture system records the trials at a sampling rate of 100 Hz. Subjects rest after each session to minimize fatigue. Based on the recorded shoulder, elbow and wrist positions (denoted by P_s, P_e and P_w respectively), trajectories of the four joint angles were computed by inverse kinematics (see Fig. 3a). These trajectories were normalized relative to the percentage of the path length traversed by the hand (instead of time) and averaged over five repetitions.

III. Results

We perform statistical tests to study whether our features are able to distinguish the behavior changes of the paretic/non-paretic arms in unimanual/bimanual modes, and to measure the inter-arm coupling strength at different joints. Fig. 4 shows representative mapping plots for Mapping 1-4. Statistical tests further compare the distribution of

the features among the joint angles, and between unimanual/bimanual modes, in two comparisons (see Fig. 3b).

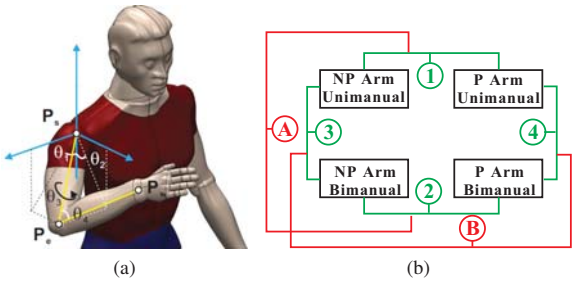

(a) (b)

Fig. 3: (a) The four joint angles extracted from the reaching motions are the shoulder abduction (θ_1), shoulder flexion (θ_2), shoulder rotation (θ_3) and elbow flexion (θ_4). (b) Mapping symmetry and complexity features are extracted from the motion mappings of non-paretic (NP) arm and paretic (P) arm, denoted by numbers, for further comparisons denoted by letters.

Two-way ANOVA are used to compare among joints and between unimanual/bimanual modes. With 95% confidence level, significant differences are found among different joints in all the four mapping features, regardless of the motion modes and motor function of the arms, which are further investigated in the multiple comparison shown in Fig. 5. Only a few significant differences were found between motion modes (in Comparison A) and between non-paretic and paretic arms (in Comparison B), presented in Fig. 5e to 5h.

IV. Discussion

A. Effect of Inter-arm Coupling on Arm Motion Symmetry

In both unimanual and bimanual modes, shoulder flexion θ_2 is the most symmetric joint. As shown in Fig. 5a and 5b, it has closest to ideal p_1 and p_2, significantly highest R^2 and lowest N_c. On the other hand, at both shoulder rotation θ_3 and elbow flexion θ_4, the paretic arm traverses less of the joint space ($p_1 < 1$) and has higher average arm posture (large positive p_2) than the non-paretic arm. Shoulder abduction θ_1 is comparable to shoulder flexion θ_2 for its p_1 and p_2, yet its R^2 and N_c are as bad as shoulder rotation θ_3 and elbow flexion θ_4. Comparison A further reveals that the symmetry at the shoulder flexion θ_2 is improved when both arms move together. In Fig. 5e, p_2 is increased at θ_2, while its mean is close to zero, which means that in unimanual mode, the paretic arm has lower average arm posture than the non-paretic arm, while in bimanual mode, the two arms have about the same posture. Such results imply that **the effect of inter-arm coupling depends on the task relevance of joints**. The task of reaching forward to touch the targets demands more motion at the shoulder flexion θ_2, while the shoulder abduction θ_1 and rotation θ_3 are less task-relevant. Human motor control generally emphasizes the control of task-relevant joints, while loosely monitoring task-irrelevant joints [22]–[24]. Consistent with this general strategy of human motor control, inter-arm coupling imposes stronger motion synchronization effort at task-relevant joints.

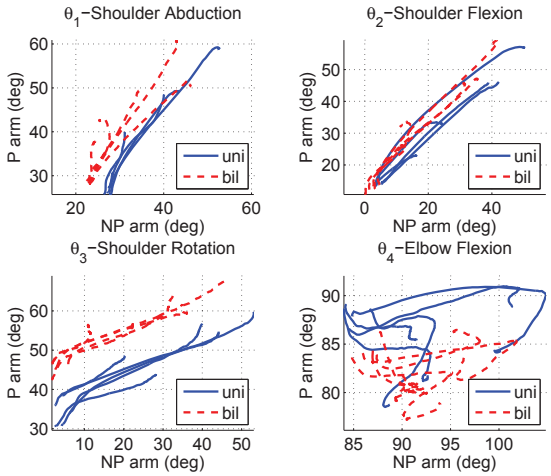

(a) From non-paretic arm to paretic arm.

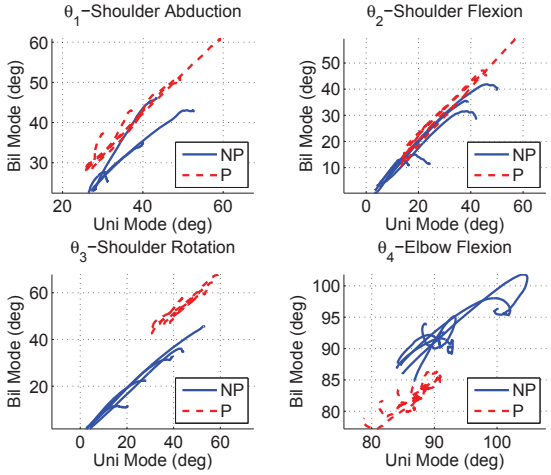

(b) From unimanual mode to bimanual mode.

Fig. 4: Representative mapping plots from a stroke subject. Given the mappings illustrated in Fig. 3b, in (a), blue solid lines refer to Mapping 1, while red dotted lines refer to Mapping 2; in (b), Blue solid lines refer to Mapping 3, while red dotted lines refer to Mapping 4.

B. Effect of Inter-arm Coupling on Arm Behavior Change

The inter-mode behavior changes of the paretic and non-paretic arms are shown in the multiple comparison among the joints in Fig. 5c and 5d. Shoulder flexion θ_2 is outstanding for highest R^2 and lowest N_c for both arms. Comparison B found significant differences between the paretic and non-paretic arms: at θ_2, the paretic arm traverses about the same distance in joint space (p_1 is about 1) and maintains about the same average arm posture (p_2 is about zero) for different modes, while the non-paretic arm traverses more of the joint space (p_1 is about 1.1) and reduces the average arm posture ($p_2 < 0$) in bimanual mode (see Fig. 5f to 5g). This indicates **the non-paretic arm contributes more to the improved motion symmetry in bimanual mode**.

Note that the paretic arm has higher posture in bimanual mode than in unimanual mode at the shoulder rotation θ_3 and elbow flexion θ_4 (see Fig. 5d for p_2), which indicates that

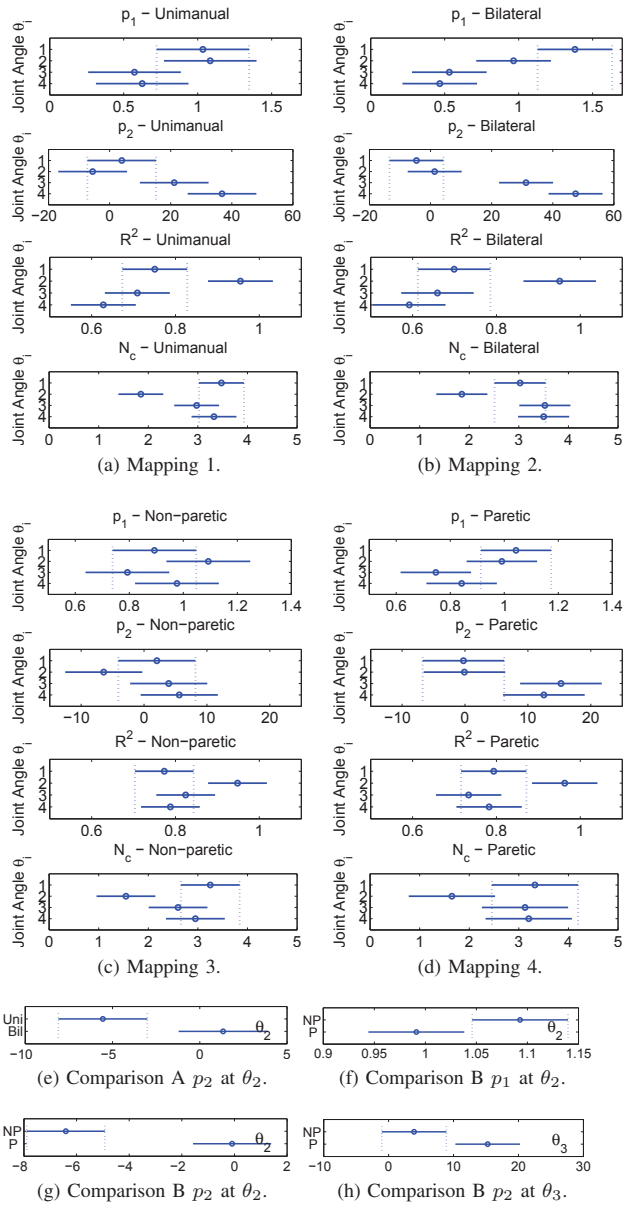

(a) Mapping 1. (b) Mapping 2.

(c) Mapping 3. (d) Mapping 4.

(e) Comparison A p_2 at θ_2. (f) Comparison B p_1 at θ_2.

(g) Comparison B p_2 at θ_2. (h) Comparison B p_2 at θ_3.

Fig. 5: Results of multi-comparison among joints (a-d). For comparisons between inter-arm mappings (Comparison A) and intern-mode mappings (Comparison B), only significant differences are displayed (e-h).

inter-arm coupling is changing the behavior of the paretic arm. Comparison B further shows that at θ_3, the increase of arm posture is significantly more pronounced in the paretic arm than the non-paretic arm (see Fig. 5h). At the same time, at the shoulder flexion θ_2, the paretic arm maintains its posture in bimanual mode, while the non-paretic arm significantly reduces its posture (see Fig. 5g). Such results suggest that **inter-arm coupling affect the behavior of both arms differently**: the paretic arm suppresses the shoulder flexion the non-paretic arm, while the non-paretic arm encourages the shoulder rotation of the paretic arm, both of which result in synchronization of motion tendency.

REFERENCES

[1] J. Kelso, D. Southard, and D. Goodman, "On the coordination of two-handed movements," *J. Exp. Psychology*, vol. 5, pp. 229–238, 1979.

[2] R. Carson, "The dynamics of isometric bimanual coordination." *Exp Brain Res.*, vol. 105, no. 3, pp. 465–76, 1995.

[3] S. Swinnen, K. Jardin, S. Verschueren, R. Meulenbroek, L. Franz, N. Dounskaia, and C. Walter, "Exploring interlimb constraints during bimanual graphic performance: effects of muscle grouping and direction." *Arch Phys Med Rehabil*, vol. 90, no. 1, pp. 79–87, 1998.

[4] M. Rice and K. Newell, "Upper-extremity interlimb coupling in persons with left hemiplegia due to stroke," *Arch Phys Med Rehabil.*, vol. 85, no. 4, pp. 629–34, 2004.

[5] M. Harris-Love, S. McCombe-Waller, and J. Whitall, "Exploiting interlimb coupling to improve paretic arm reaching performance in people with chronic stroke," *Arch Phys Med Rehabil*, vol. 86, no. 11, pp. 2131–7, 2005.

[6] D. Rose and C. Winstein, "The co-ordination of bimanual rapid aiming movements following stroke," *Clin Rehab*, vol. 19.

[7] B. Bobath, *Adult hemiplegia: evaluation and treatment. 3rd ed.* Oxford: Butterworth-Heinemann, 1990.

[8] M. Mudie and T. Matyas, "Can simultaneous bilateral movement involve the undamaged hemisphere in reconstruction of neural networks damaged by stroke?" *Disabil. Rehab.*, vol. 22.

[9] J. Whitall, S. McCombe Waller, K. Silver, and R. Macko, "Repetitive bilateral arm training with rhythmic auditory cueing improves motor function in chronic hemiparetic stroke," *Stroke*, vol. 31, no. 10, pp. 2390–5, 2000.

[10] J. Cauraugh and S. Kim, "Two coupled motor recovery protocols are better than one: electromyogram-triggered neuromuscular stimulation and bilateral movements," *Stroke*, vol. 33, no. 6, pp. 1589–94, 2002.

[11] M. Stoykov and D. Corcos, "A review of bilateral training for upper extremity hemiparesis." *Occup Ther Int.*, vol. 16.

[12] G. Lewis and W. Byblow, "Neurophysiological and behavioural adaptations to a bilateral training intervention in individuals following stroke," *Clin Rehabil*, vol. 18, no. 1, pp. 48–59, 2004.

[13] J. Desrosiers, D. Bourbonnais, H. Corriveau, S. Gosselin, and G. Bravo, "Effectiveness of unilateral and symmetrical bilateral task training for arm during the subacute phase after stroke: a randomized controlled trial," *Clin Rehabil*, vol. 19, no. 6, pp. 581–93, 2005.

[14] C. Peper, P. Beek, and P. van Wieringen, "Frequency-induced phase transitions in bimanual tapping." *Biol Cybern.*, vol. 73.

[15] S. Swinnen and N. Wenderoth, "Two hands, one brain: Cognitive neuroscience of bimanual skill," *Trends in Cognitive Science*, vol. 8, no. 2004, pp. 18–25, 2004.

[16] H. Heuer, W. Spijkers, T. Kleinsorge, H. van der Loo, and C. Steglich, "The time course of cross-talk during the simultaneous specification of bimanual movement amplitudes." *Exp Brain Res.*, vol. 118, pp. 381–92, 1998.

[17] L. Bagesteiro and R. Sainburg, "Handedness: dominant arm advantages in control of limb dynamics." *J Neurophysiol.*, vol. 88, pp. 2408–21, 2002.

[18] K. Haaland, J. Prestopnik, R. Knight, and R. Lee, "Hemispheric asymmetries for kinematic and positional aspects of reaching." *Brain*, vol. 127, pp. 1145–58, 2004.

[19] H. Heuer, "Control of the dominant and nondominant hand: exploitation and taming of nonmuscular forces." *Exp Brain Res.*, vol. 178, no. 3, pp. 363–73, 2007.

[20] R. Sainburg, "Evidence for a dynamic-dominance hypothesis of handedness." *Exp Brain Res.*, vol. 142, pp. 241–58, 2002.

[21] N. Dounskaia, K. Nogueira, S. Swinnen, and E. Drummond, "Limitations on coupling of bimanual movements caused by arm dominance: when the muscle homology principle fails." *J. Neurophysiol.*, vol. 103, no. 4, pp. 2027–38, Apr. 2010.

[22] J. P. Scholz and G. Schoner, "The uncontrolled manifold concept: identifying control variables for a functional task," *Experimental brain research*, vol. 126, no. 3, pp. 289–306, 1999.

[23] M. Latash, *Synergy*. Oxford University Press, USA, 1 edition, 2008.

[24] Z. Li, J. Roldan, D. Milutinovic, and J. Rosen, "Task-relevance of grasping-related degrees of freedom in reach-to-grasp movements," in *Conf Proc IEEE Eng Med Biol Soc.*, Chicago, IL, Aug. 2014, pp. 6903–6.